Supplementary Information (SI) for Sustainable Energy & Fuels.

Supplementary Information

The negative graphite electrode was found to be highly oriented: the c-axis (normal to the graphite sheets) was found to have a preferred orientation perpendicular to the current collector. In the diffraction ring patterns acquired during the experiment (**Fig. S1a)**, there is a preferred orientation texture in the sample. In fact, the overall pattern of the diffraction rings may show a systematic arrangement of intensities, indicating a preferential orientation texture within the powder sample. This texture can manifest as a pattern of alternating strong and weak diffraction intensities around the ring. From the change of intensity of the graphite reflection, it is clear that there is a strong horizontal orientation of the crystallographic planes.

Fig. S1b shows the NMC 003 reflection intensity and the 002 graphite reflection intensity as a function of the azimuthal angle eta (η) of the ring pattern **(Fig.1b)**. The NMC showed a constant intensity, i.e. a random orientation. On the other hand, the graphite showed a higher intensity close to 0 and 180 degrees.

Fig. S2 shows the 002 graphite reflection intensity distribution and the intersection with the planes along which the 002 was measured.
If an azimuthal integration is used on a sample that is strongly anisotropic, the reconstructed image will show significant artifacts such as an intensity gradient. Fig.S3 shows the tomographical reconstruction image of graphite (a) and NMC (c) inside the 18650 when all the η range in the powder diffraction ring was used for the reconstruction. Since NMC is randomly oriented, no intensity gradient can be observed. On the other end, the graphite reconstruction shows a significant radial intensity gradient, where the intensity of the signal decreases significantly in the centre. This is not due to a lack of material but can be related to a strong artifact since the signal is not invariant for rotation due to the preferential orientation. When the reconstruction of graphite is made with just scattering from azimuthal range of integration $\eta=\pm15°$, there are no circular gradients present towards the centre of the cell, indicating a signal that does not vary with rotation and therefore, acceptable for tomographical reconstruction.

Figure S4 shows the shows the distribution (in a.u.) of the graphite c-axis orientations (black) and NMC (blue) as function of η. The graphs express the statistical distribution of the orientation of the c-axis (normal to the sheets) in different planes. The orientation of the c-axis in the graphite cell is primarily perpendicular to the current collector, along the radial direction, with a small fraction of the c axis oriented parallel to the current collector sheet. While the NMC does not show any preferential orientation.
Figure S7 shows the comparison of lithiation distribution inside the negative electrode in pristine (fig A-J) and aged cell (fig K-T) during discharge. Same heterogeneities found during charge in the aged cell were confirmed during discharge.

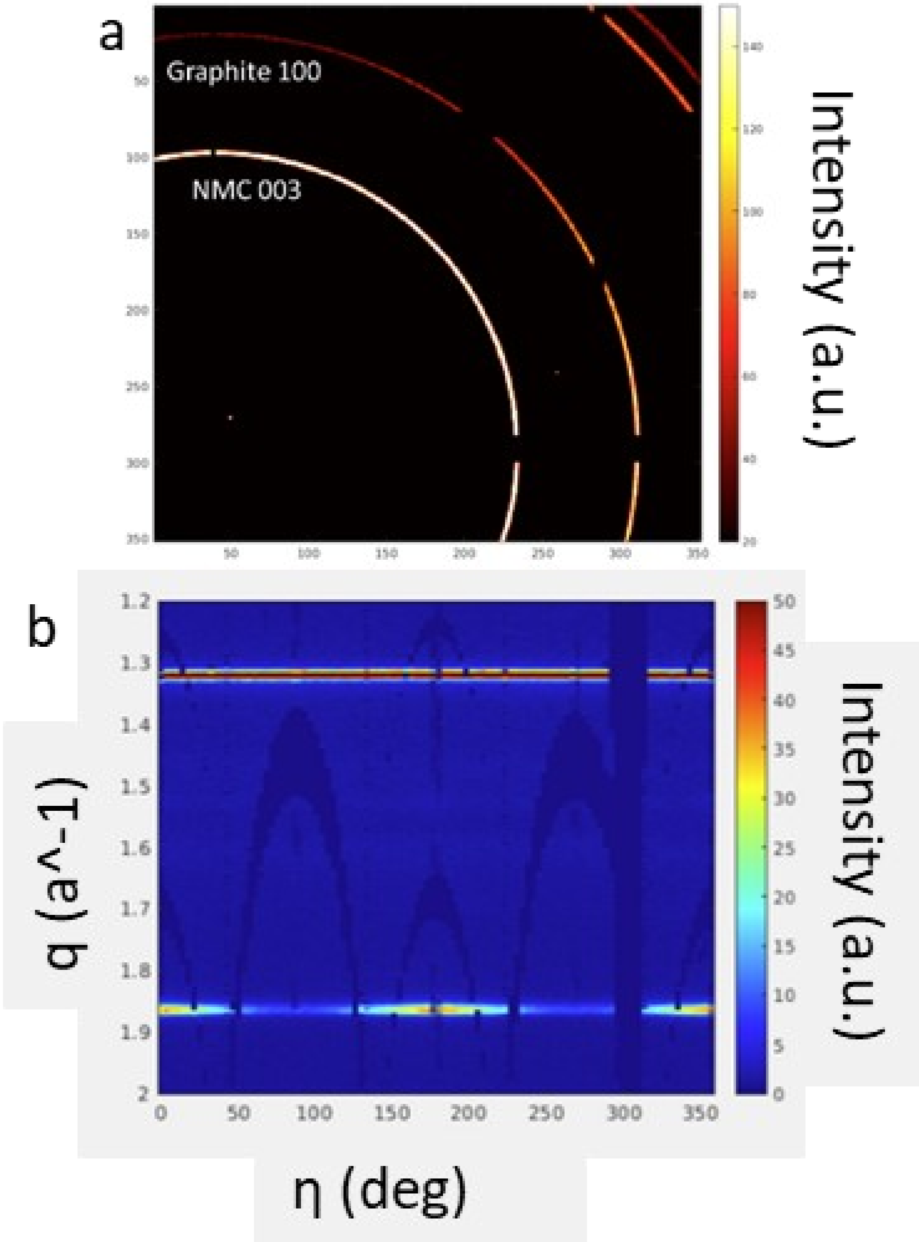

Figure S1 a, diffraction ring of 18650 cell in the discharged state. The first ring closer to the centre is the NMC 003 reflection, showing a homogenous intensity. The second ring is the graphite 100 reflection. The graphite shows a horizontal preferential orientation due to its higher intensity closer to 180 degrees. B, polar transformation of a: NMC 003 reflection intensity(1.32q) and the 002 graphite reflection intensity(1.87q) acquired during the experiment. In the graph, the intensity is plotted as function of azimuthal angle eta(η) of the ring pattern.

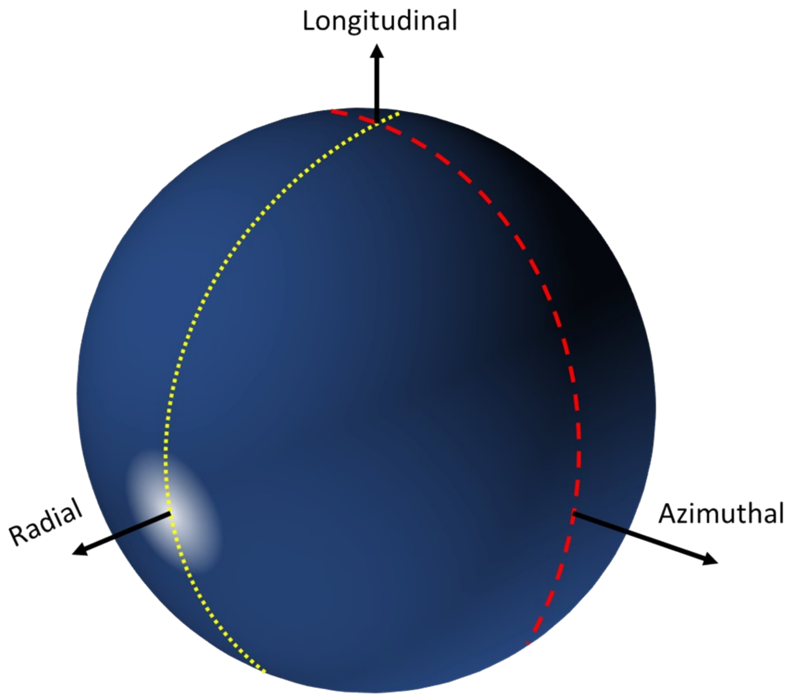

Figure S2 the 002 graphite reflection intensity distribution and the intersection with the planes along which the 002 was measured.

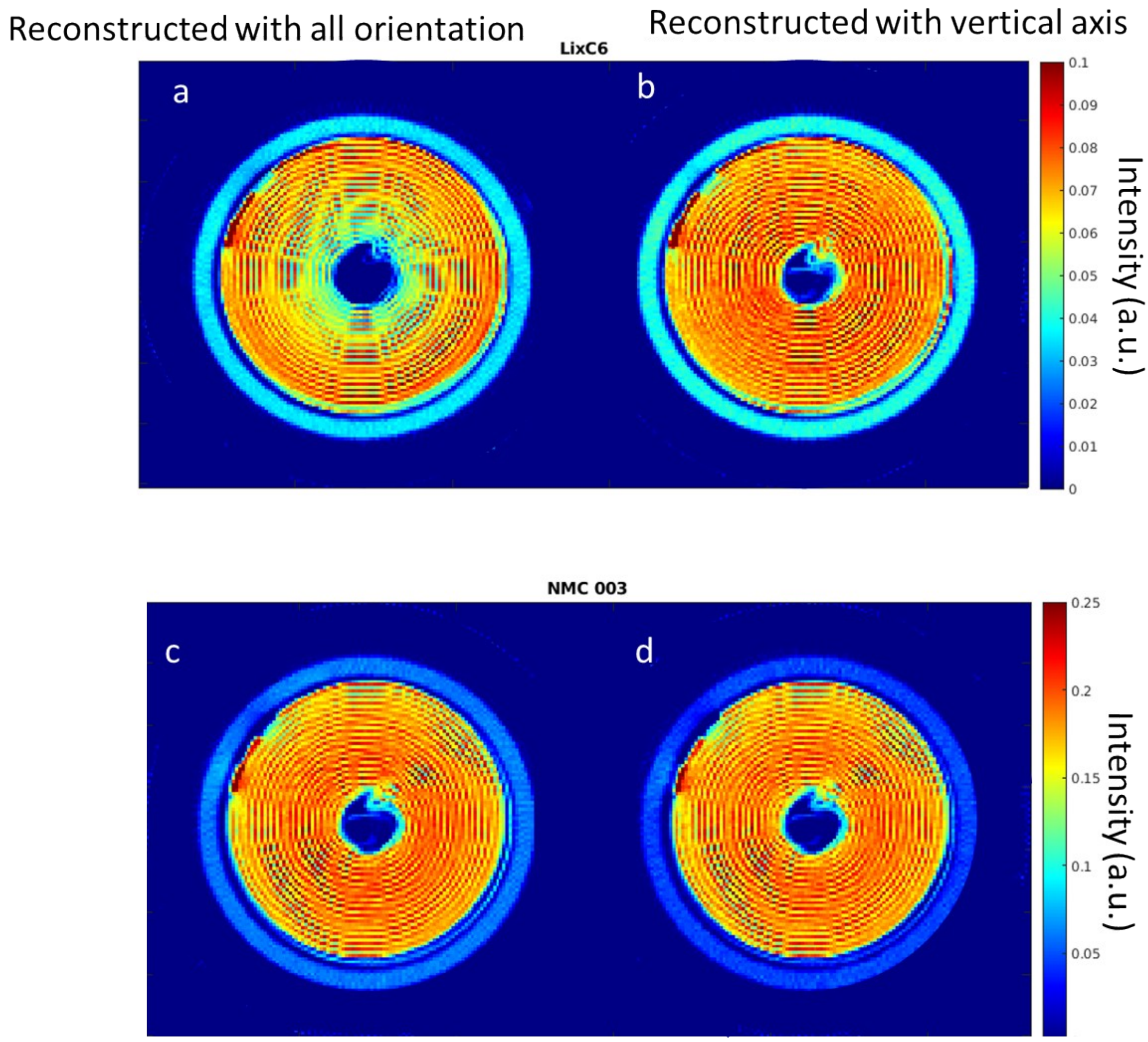

Figure S3 Example of tomographical reconstruction of a. Graphite using the entire powder diffraction scattering, b. Graphite using only signal integrated with η=±15, c. 003 NMC reflection using the entire powder diffraction scattering, d. 003 NMC reflection using only signal integrated with η=±15.

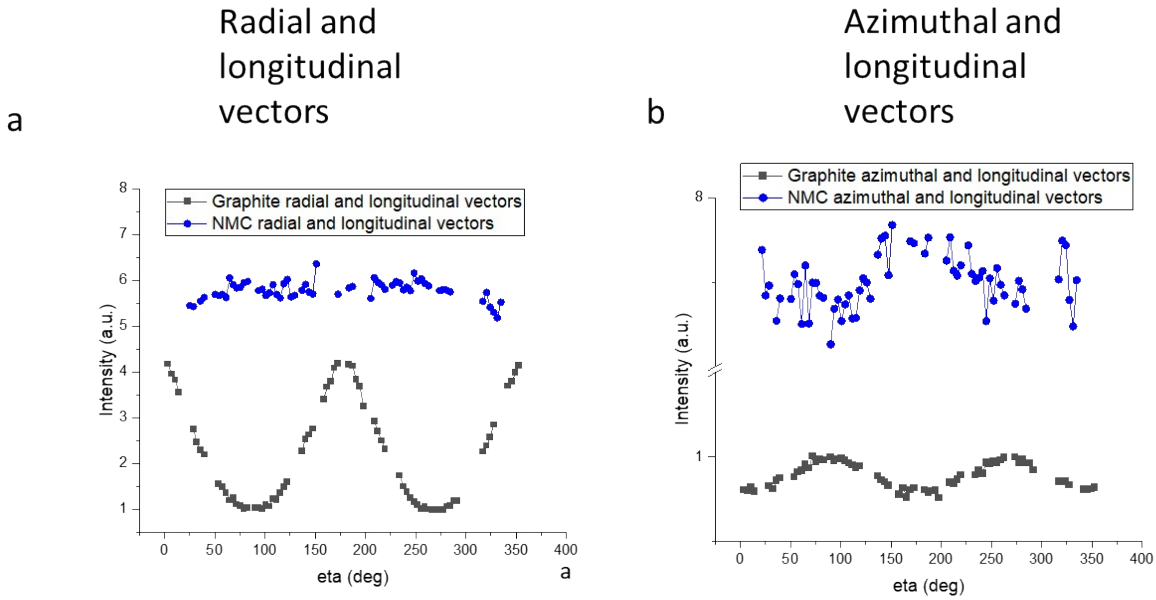

Figure S4 The two graphs represent the statistical distribution of the 003 NMC reflection (red) and 002 graphite reflection (black) in different planes. a, the distribution in the plane defined by the radial and longitudinal direction of cell. B, the distribution in the plane defined by the longitudinal and azimuthal directions of the pristine cell.

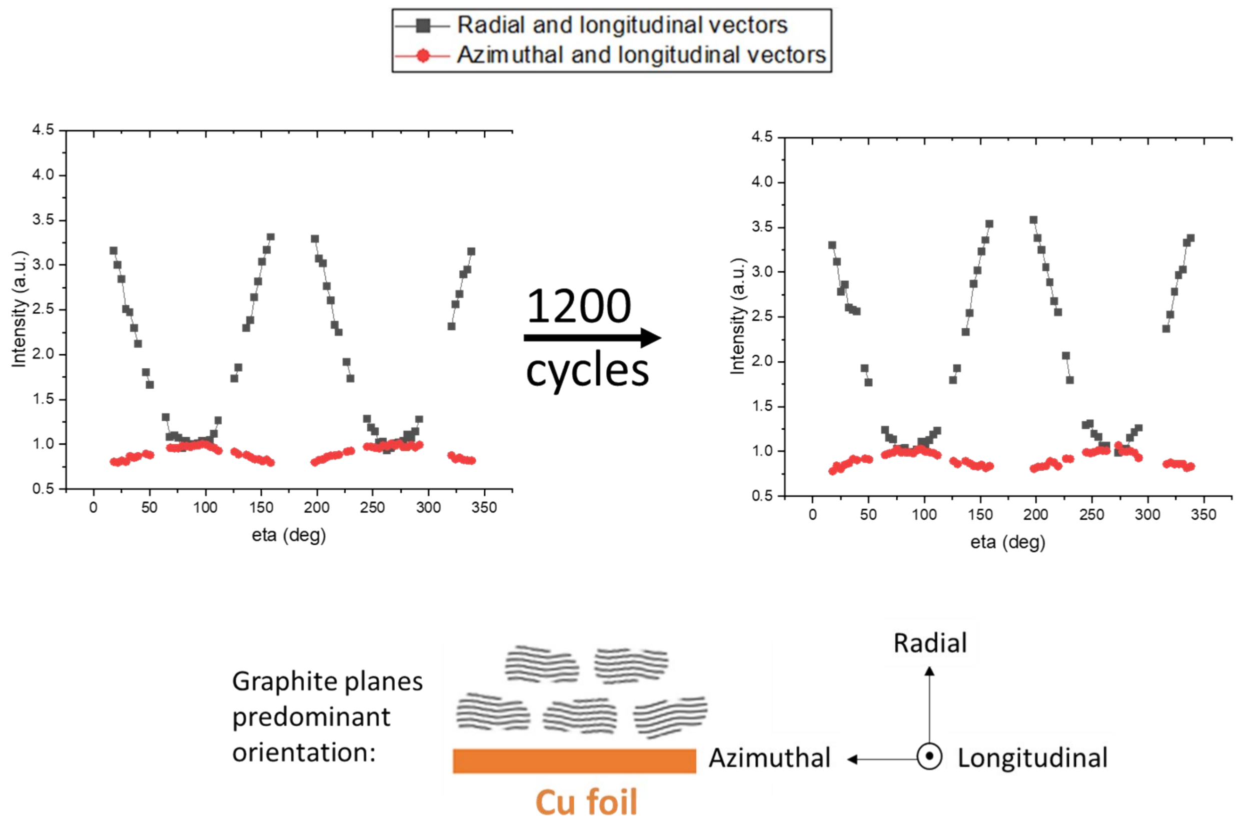

Figure S5 The graphs represent the statistical distribution of the orientation of the c-axis (normal to the graphite sheets) in different planes in the charged state. The black square graphs show the distribution in the plane defined by the radial and longitudinal direction of pristine (left) and aged cell (right). The red circle graphs show the distribution in the plane defined by the longitudinal and azimuthal directions of pristine (left) and aged cell (right).

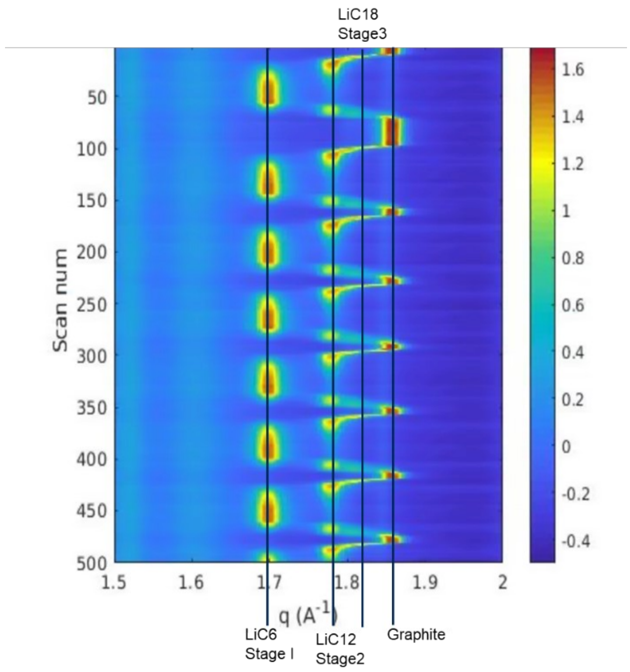

Figure S6 Bragg's peaks of different graphite lithiation stages as function of q at different scan numbers during cycling.

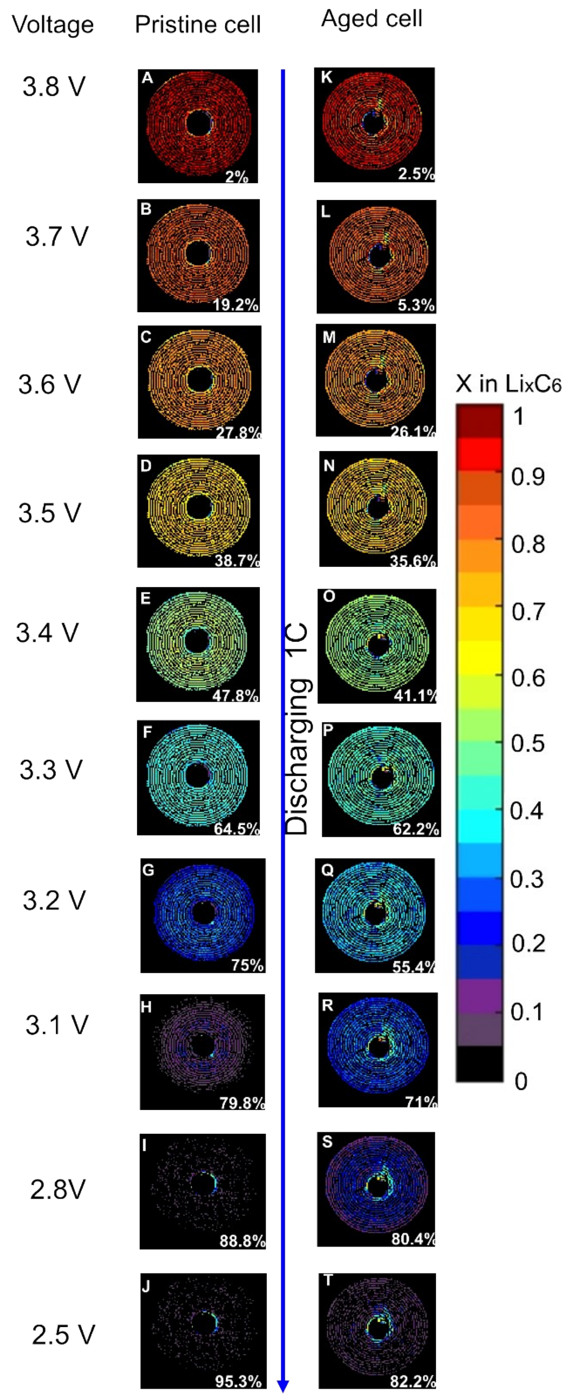

Figure S7 Comparison of lithiation distribution inside the negative electrode in pristine (fig A-J) and aged cell (fig K-T) during discharge. The lithiation distribution is analysed during a CC discharge cycle at 1C for each cell. Fig. A-T show the distribution of x in LixC6 as function of a coloured bar (shown on the right). Black corresponds to C6 delithiated graphite, red corresponds to LiC6 fully lithiated state. The voltage at which the distribution is analysed is shown on the left, while the cell capacity at which the XRD-CT corresponds to is on the bottom right of each image from A-T.